Stanford Exploration Project, Report 95, October 10, 1997, pages 265–283

Stanford Exploration Project, Report 95, October 10, 1997, pages 265–283

An anisotropic Marmousi model

Tariq Alkhalifah[1]

keywords: *anisotropy, modeling*

ABSTRACT

I use the acoustic wave equation for transversely isotropic media with vertical symmetry axis (VTI media), to generate synthetic VTI data for an anisotropic version of the Marmousi model. This acoustic equation, though it represents a physically impossible medium, provides an extremely accurate approximation of the widely used elastic wavefield. The anisotropic Marmousi model has the same NMO velocity as the original Marmousi model and an anisotropy η distribution that possesses the same layering characteristics as the velocity model. Interval η spans the range of 0 to 0.27, which are values that are commonly observed in practice. The traveltime and amplitude differences between the synthetic seismograms of this new anisotropic model and those produced by the original isotropic Marmousi data set are quite apparent. As a result, a prestack isotropic migration failed to properly image the anisotropic data when using the exact original velocity model.

INTRODUCTION

The Marmousi model has become synonymous with the phrase *complex media*. The huge amount of folding and faulting induced in this model have created a rather interesting distribution of velocity anomalies and discontinuities. Thus, the Marmousi model served as a calibration tool (Audebert et al., 1994; Versteeg and Lailly, 1991; Rekdal and Biondi, 1994) used to test the various traveltime and migration algorithms through the years.

One of the biggest contributions of the Marmousi model is that it demonstrated the limitations of first-arrival traveltimes in imaging complex media. Specifically, Geoltrain and Brac (1993) showed that to properly image the Marmousi model we need multi-arrival traveltimes. In portions of the Marmousi model, or any other complex model, the first arrival is not necessarily the most energetic. Therefore, reflected energy from key horizons, such as the top of the reservoir, are not properly imaged by using only first arrival traveltimes.

[1]**email:** tariq@sep.stanford.edu

The Marmousi data set was generated at the Institute Francais du Petrole (IFP), and used for the workshop on practical aspects of seismic data inversion at the 1990 EAEG meeting in Copenhagen, where different groups (contractors, universities, and oil companies) applied their proffered imaging tools on this data set. Detailed accounting of what transpired at the workshop is given by Versteeg and Grau (1990) and Versteeg and Lailly (1991). The original Marmousi data set was generated using a 2-D acoustic finite-difference modeling program. The Marmousi model is, however, based on the simplistic assumption that the Earth subsurface is isotropic, despite the many arguments (Banik, 1984; Harris et al., 1994) that suggest otherwise.

In an accompanying paper (Alkhalifah, 1997d), I derive an acoustic wave equation for transversely isotropic media with a vertical symmetry axis (VTI media). This equation is fourth order and, as a result, has four solutions. Two of those solutions are the P-wave solutions for incoming and outgoing waves. The other two are artifacts of the formulation that can be easily avoided by placing the receivers in an isotropic layer. This equation can be used to simulate wave propagation in VTI media using finite difference schemes.

The existence of such an acoustic wave equation allows us to generate realistic synthetic data in complex models. An example of a complex model is the ever popular Marmousi model. Although this geological model is based on a somewhat accurate expectation of the subsurface in certain Earth regions, as mentioned above, it lacks the recognition of the possible anisotropy that shales often induce in seismic waves. Unlike inelasticity, anisotropy effects seismic wave traveltimes, and in some cases, this effect is large enough to cause major traveltime differences. By ignoring anisotropy, the conventional velocity interpretation becomes biased toward typically higher velocity values in the case in which $\eta > 0$.

Building an anisotropic Marmousi model allows us to examine the advantages as well as the drawbacks of the various methods used to calculate traveltimes in VTI media. Although the conclusions might be similar to those observed in isotropic media, these tests will give some insight into how much anisotropy might affect conventional processing.

In this paper, I outline the steps taken to build the anisotropic Marmousi model and generate synthetic seismograms using the VTI acoustic wave equation. I show snapshots of the wavefield at various times and highlight differences between the new anisotropic data set and the original isotropic one. An isotropic migration of the new anisotropic data reveals some of the drawbacks of ignoring anisotropy.

THE THEORY

Four parameters govern wave propagation in general elastic transversely isotropic media with a vertical symmetry axis (Aki and Richards, 1980). In a recent paper (Alkhalifah, 1997), I have showed that only three are needed to totally characterize P-wave propagation in acoustic VTI media. Although an acoustic VTI medium does not physically exist, it provides, like its isotropic counterpart, exceptionally accurate kinematic representation of wave propagation in elastic media. It also accurately characterizes the geometrical amplitude behavior of the wave propagation. The only drawback of the acoustic assumption is its inaccurate description of transmission and reflection behavior of waves in true elastic conditions.

The three parameters needed to characterize the acoustic model in VTI media are the vertical P-wave velocity, v_v, the normal moveout (NMO) velocity for a horizontal reflector (Thomsen, 1986), v, and an anisotropy parameter denoted by η. This anisotropy parameter is related to the horizontal velocity, v_h, (Alkhalifah and Tsvankin, 1995) as follows:

$$\eta = \frac{1}{2}\left(\frac{v_h^2}{v^2} - 1\right). \tag{1}$$

If η=0 the medium is elliptically anisotropic, and if we set v_v=v, the medium eventually become isotropic. Typical η values in the subsurface range from 0 to 0.3 (Alkhalifah, 1997a).

Conveniently, in a recent paper (Alkhalifah, 1997d), I derived a wave equation based on the acoustic assumption for VTI media. Taking P as the wavefield, this equation in two-dimensional (2-D) media is

$$\frac{\partial^2 P}{\partial t^2} = (1+2\eta)v^2\frac{\partial^2 P}{\partial x^2} + v_v^2\frac{\partial^2 P}{\partial z^2} - 2\eta v^2 v_v^2 \frac{\partial^4 F}{\partial x^2 \partial z^2} + f, \tag{2}$$

with

$$P = \frac{\partial^2 F}{\partial t^2}, \tag{3}$$

where $f(x,z,t)$ is the force function, and x and z are variables of the 2-D Cartesian coordinate system.

Equation (2) is fourth order in time and as such, has four solutions. Two of them are the conventional P-wave solutions for incoming and outgoing waves. The other two solutions represent artifacts of the new formulation and thus are unwanted. They are also conjugate solutions that tend to grow exponentially for negative η, and behave like propagating waves for positive η. Luckily, these waves, or artifacts, do not travel in isotropic media. Therefore, they can be eliminated by placing the receivers in an isotropic layer. For marine-type surveys, the receivers are commonly placed in the water layer which is conveniently isotropic (Alkhalifah, 1997d). This is also the case for the Marmousi model, which includes a thin shallow water layer.

THE MODEL

The original Marmousi model was built to resemble an overall continental drift geological setting. Numerous large normal faults were created as a result of this drift. The geometry of Marmousi is based somewhat on a profile through the North Quenguela through the Cuanza basin (Versteeg, 1993). The target zone is a reservoir located at a depth of about 2500 m. The model contains many reflectors, steep dips, and strong velocity variations in both the lateral and the vertical direction (with a minimum velocity of 1500 m/s and a maximum of 5500 m/s). However, there is no clear evidence of the Marmousi model intended sediment or rock distribution, and this includes the distribution of shales. As a result, the same discard for sediment distribution, that went into building the sediment content of the original model, is used here. This is justified by the fact that our goal is purely imaging. Nobody seemed to care for the geological aspect of the model.

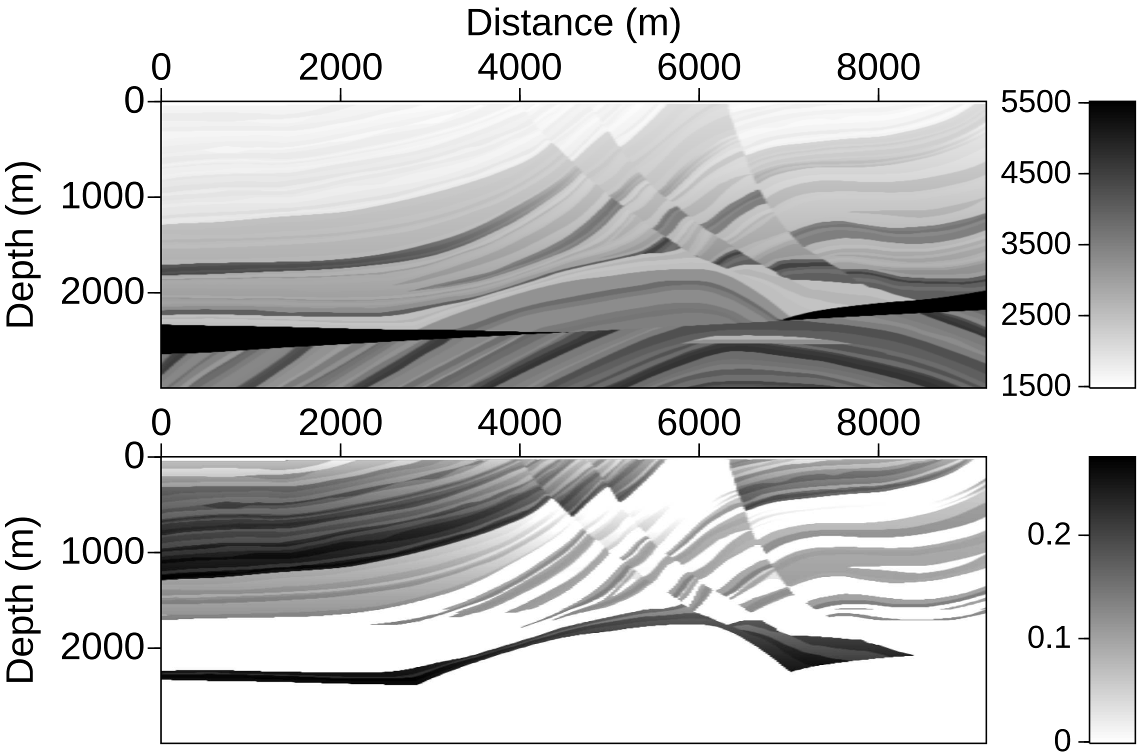

Figure 1: Top: The original Marmousi velocity model given by IFP. Bottom: An η model built using the above Marmousi velocity model and constraining the horizontal velocity to increase linearly. The values of η range from zero to 0.274. The vertical P-wave velocity for this VTI model is taken to equal v, shown on top. tariq3-veleta [NR]

Figure 1 (top) shows the original velocity model used by the Institute Francaise du Petrole (IFP) to generate the Marmousi synthetic data set. Figure 1 (bottom) shows an η model that is based on the following two hypothetical assumptions:

- Anisotropy increases as velocity decreases (shales have low velocity overall).
- The horizontal velocity gradually increases with depth.

The second assumption means that although the NMO velocity may vary erratically, the horizontal velocity retains a relatively linear increase with depth. Although there is no settled proof that the above assumptions are accurate representation of the subsurface behavior in the presence of anisotropy, my personal experience suggests that they are at least plausible. Nevertheless, my goal is not to build a realistic geological model, but rather to obtain anisotropic data from a complex model that we can use to test existing anisotropic algorithms.

As mentioned in the previous section, three parameters describe wave propagation in an acoustic VTI model. The parameter η is perhaps the most influential with respect to the anisotropic influence on imaging and focusing (Alkhalifah and Tsvankin, 1995). On the other hand, v_v is responsible for the depth positioning of reflectors. In this model, v_v is set to equal the NMO velocity, v, because theoretically v_v is unresolvable from surface P-wave seismic data (Alkhalifah, 1997; Alkhalifah et al., 1997). It can only be obtained from well data, and such information is beyond the scope of this paper. Apart from the imaging issue, fitting an isotropic model to anisotropic data results in over-estimation of NMO velocity, and thus over-estimation of depth even if the vertical velocity equals the NMO velocity (Alkhalifah, 1997b).

For the VTI model, the NMO velocity, v, is given by the IFP original velocity model. The anisotropy parameter η is built to inherent the layering of the original IFP velocity model. This task is accomplished by imposing three guidelines on η:

- η=0 for layers with v=1500 m/s, which corresponds to the water layer.
- η=0 for layers with v >2500 m/s, which are velocities higher than those of a typical shale layer.
- η satisfies equation (1) and $v_h = 1750 + 0.8z$ m/s in all other layers of the model.

As a result, interval η, shown in the bottom panel of Figure 1 ranges from zero to 0.274, which is a practical range for η in the subsurface (Alkhalifah, 1997a,b). Specifically, η=0.274 corresponds to a difference between the horizontal to vertical P-wave velocity of about 25 percent, which is a reasonable value (Banik, 1984; Harris et al., 1994). Meanwhile, effective η (Alkhalifah, 1997b), which represents an average of the overburden η influence, has overall lower values than the interval η. It is the effective η, not the interval η, that has a direct impact on imaging.

THE WAVEFIELD

One way to examine the difference between wave propagation in isotropic and VTI media is by observing snapshots of the wavefield generated by each medium. Figure 2 shows snapshots of the wavefield at 0.65 s and 1.3 s resulting from a source near the surface at lateral position 3000 m from the origin. The source location represents the first shot point of the original Marmousi data acquisition. This source is above a more anisotropic and less complex region of the VTI Marmousi model; an ideal setting for testing nonhyperbolic and tomographically based inversions for anisotropic media; both methods excel in smooth media.

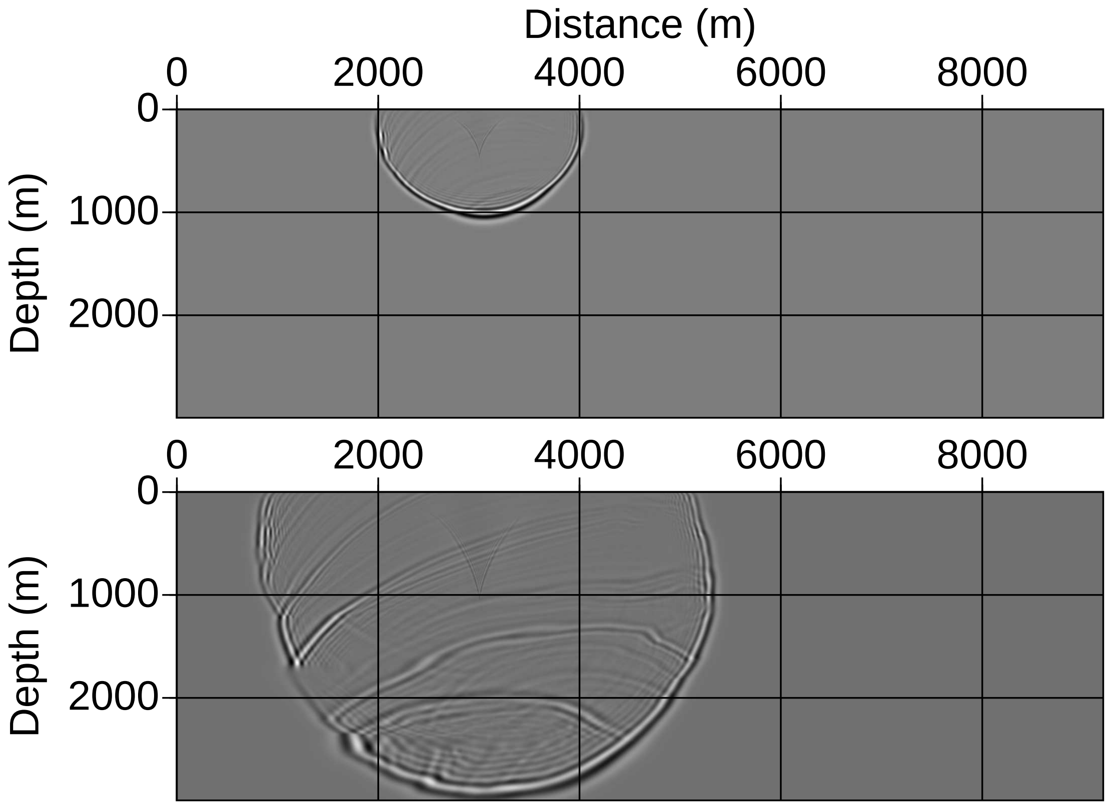

Figure 2: Snapshots of the wavefield at 0.65 s (top) and 1.3 s (bottom) resulting from a source at the 3 km position. The wavefield was generated using the new acoustic wave equation for VTI media. The velocity and η models are shown in Figure 1. tariq3-snap-marmo3000f [NR]

On the other hand, Figure 3 shows snapshots of the wavefield at 0.65 s and 1.3 s for the original isotropic Marmousi velocity model. Because the vertical velocity is the same for the anisotropic and isotropic Marmousi models, the portion of the wavefront corresponding to vertical wave propagation is similar, which we can see by subtracting the two wavefields, with results shown in Figure 4. As expected, the largest difference between the two wavefields occurs for near horizontal-direction wave propagation, where clear separation between the two fields are shown in Figure 4 in that direction. Careful observation of the difference section (Figure 4) shows that such separation is largest for waves propagating toward the origin (lower values of distance) because of the higher level of anisotropy in that region. Most energies recorded by the geophones arrive at incident angles closer to vertical than horizontal. Therefore, the large separation of energy in the horizontal direction of wave propagation in the two models is not a true indication of what to expect in the processing stage.

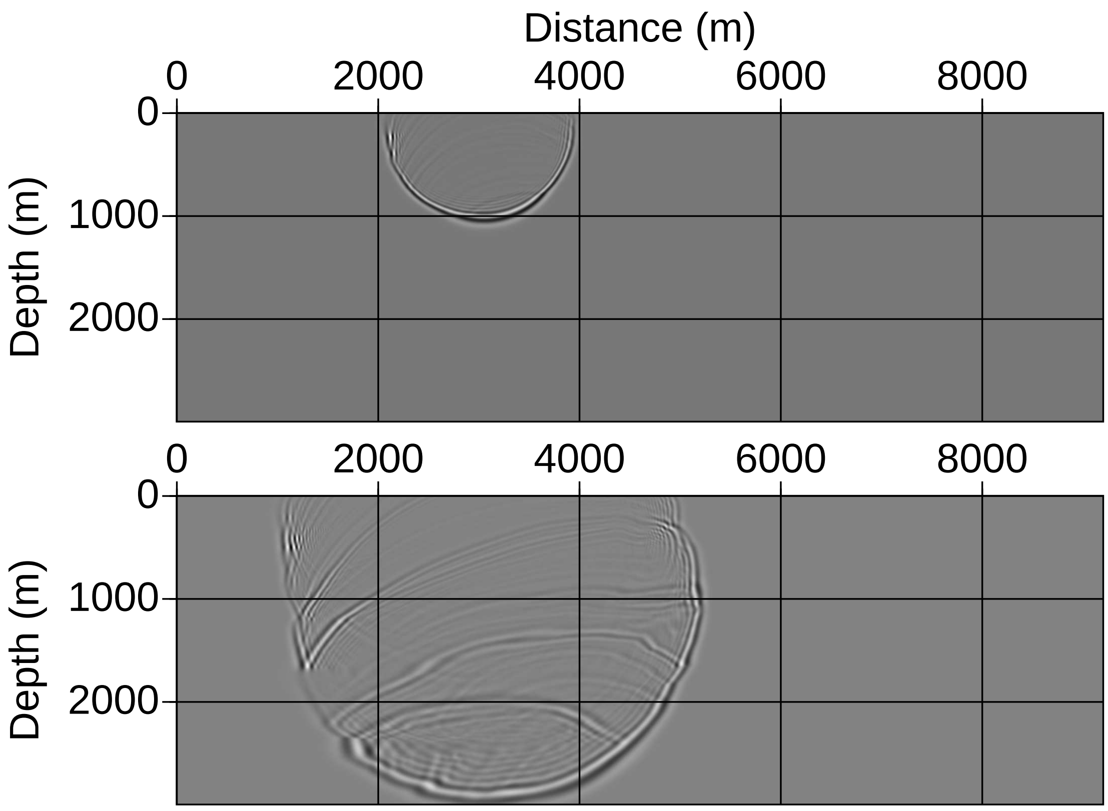

Figure 3: Snapshots of the wavefield at 0.65 s (top) and 1.3 s (bottom) resulting from a source at distance 3 km. The medium is isotropic. The velocity model is shown in Figure 1 (top). tariq3-snap-marmo3000isf [NR]

The synthetic data, discussed in the next section, should provide a better idea of what to expect in the processing stage.

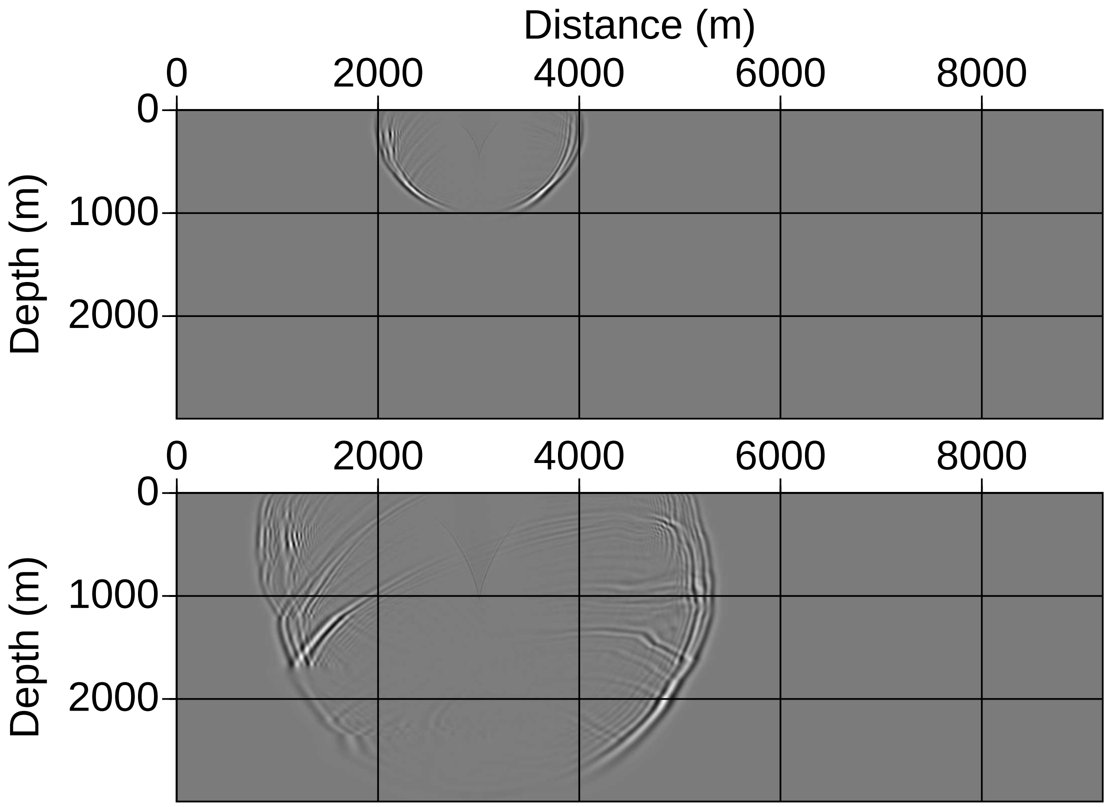

Figure 4: A plot of the difference between the sections in Figures 2 and 3, given at the same scale. tariq3-snap-marmodiff [NR]

THE SYNTHETICS

The original Marmousi data set consists of 240 shots with 96 traces per shot. The first offset is 200 m; both the shot and the receiver spacings are 25 m. The first shot is at the lateral position 3000 m, and the recording time is 2.9 s. Overall, I used the same survey geometry and settings used by IFP, the builders of the original Marmousi data set. This includes the same source and receiver locations, an identical sampling interval and recording time, and the same minimum offset.

However, I made two adjustments to the original Marmousi acquisition settings:

- The peak frequency of the new, anisotropic, data is 30 Hz (5 Hz higher than the original data), which is more consistent with survey frequencies nowadays, and corresponds a causal ricker-wavelet point source.
- The spread length was extended to include offsets up to 3575 m, as opposed to only 2575 m in the original data.

The second modification is important for anisotropic inversion, because a majority of the information on anisotropy inversion comes from large offsets. Although the general complexity of the Marmousi model makes it less than ideal for anisotropic inversion, parts of the model are potentially invertible, including the region under the surface location 3000 m. In addition, I implemented absorbing boundary conditions at all four boundaries of the model. Doing so eliminates the presence of surface multiples; however, other inter-bed multiples can exist.

Figure 5 shows a common-shot gather (the first shot of the survey) from the original Marmousi data set , on the top, and the corresponding common-shot gather for the new VTI Marmousi data, on the bottom. The moveout of most reflections at this shot point appears hyperbolic, overall, a direct indication of the smoothness of the model under this shot point location. The reflection at two seconds might be the only exception. Head waves, which are the first arrivals at moderate to large offsets, are faster for the VTI case than for the isotropic case. The difference of 0.2 s, or 12 percent, is directly attributable to the average η value of about 0.15 near the surface in that shot-point area. In addition, all reflections at far offsets arrive much earlier in the anisotropic model than the isotropic one, despite the fact that the two models have the same NMO velocity. We can attribute these differences mainly to the nonhyperbolic moveout, commonly associated with anisotropy.

Another common-shot gather, shown in Figure 6 and caused by a source at 5000 m, demonstrates additional complications. The moveout no longer appears hyperbolic, which directly reflects the complexity of the model under this shot point. Differences between the isotropic (top) and anisotropic (bottom) sections are apparent. The diffraction at 0.7 seconds has large amplitudes in the isotropic section, and low amplitudes in the anisotropic one. We attribute this difference to the lower velocity contrast between the diffractor, which is of a high velocity, and the medium above

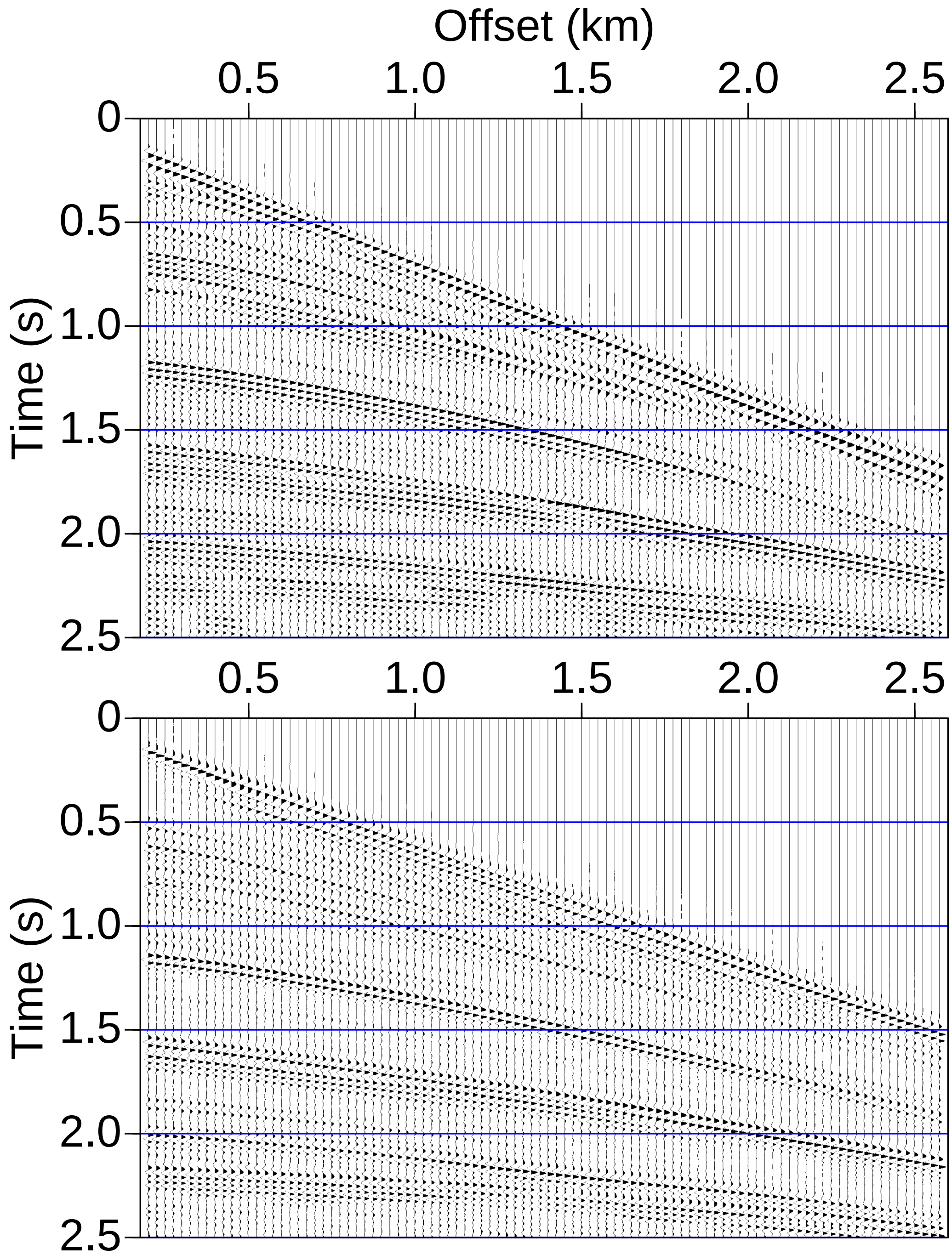

Figure 5: Common-shot gathers for the model in Figure 1 resulting from a source at the 3 km location and geophones that range from 0.2 to 2.8 km locations. Both sources and receivers are at depth 25 m from the surface. Top: Shot gather from the original Marmousi data set, based on an isotropic medium. Bottom: Shot gather computed using the new acoustic equation (2) for VTI media applied to the VTI velocity model. tariq3-syn-marmo3000 [NR]

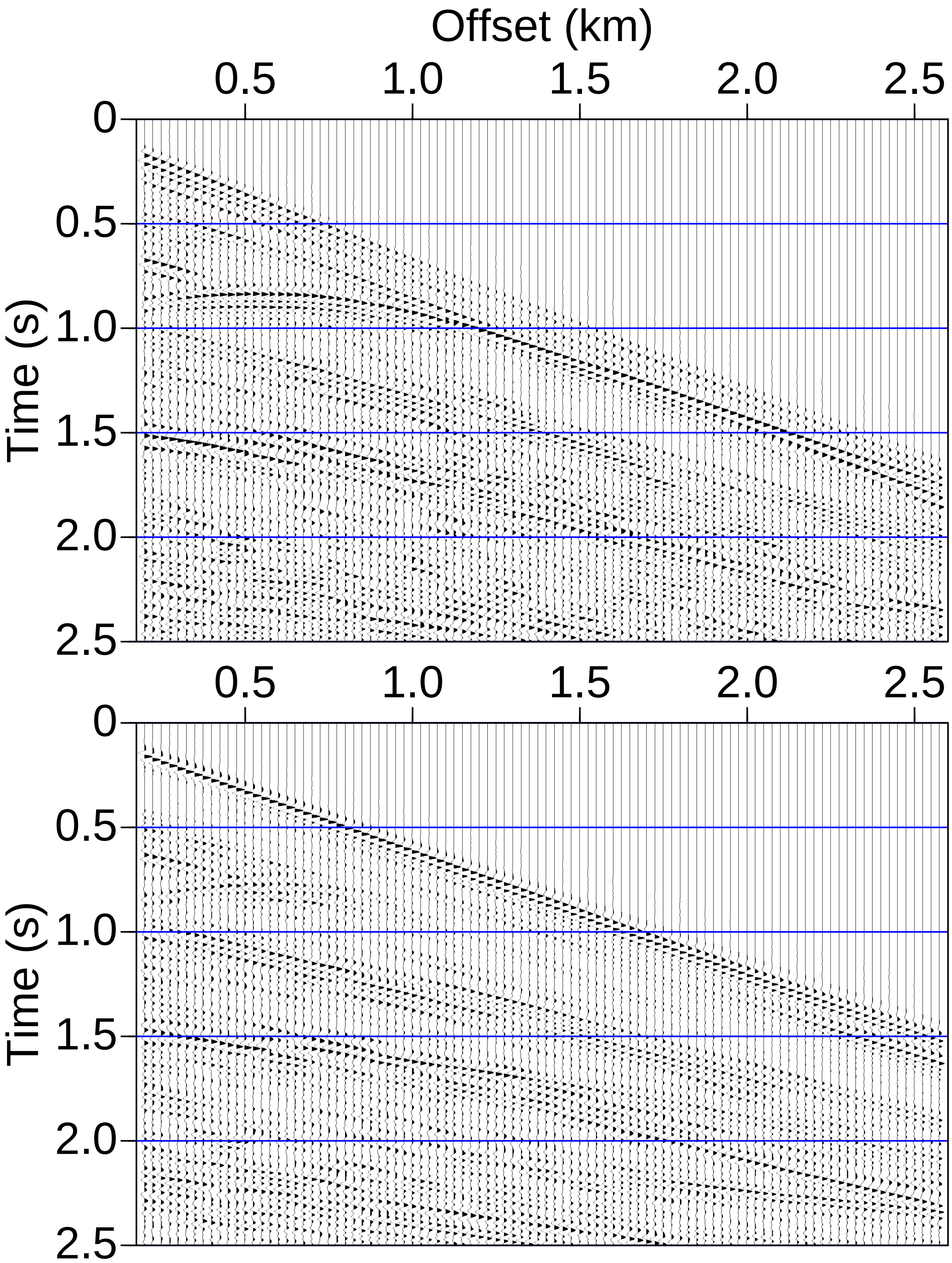

Figure 6: Common-shot gathers, similar to those in Figure 5, but the source is placed at the 5 km surface location and the geophones range from 2.2 to 4.8 km. Top: Shot gather from the original Marmousi data set, based on isotropy. Bottom: Shot gather based on the VTI model. tariq3-syn-marmo5000 [NR]

it in the anisotropic model. Such amplitude differences have large implications in amplitude-versus-offset (AVO) analysis of reflections. Well-log (vertical) velocities do not constrain the AVO behavior in anisotropic media; the parameter η is also needed to do so.

Another common-shot gather, shown in Figure 7 and resulting from a source at 7000 m, is recorded at a more isotropic, yet complex, region of the anisotropic model. The overall differences between the isotropic (top) and anisotropic (bottom) sections are smaller than those associated with Figures 5 and 6. Head waves for the isotropic and anisotropic models at far offsets arrive at less than 0.1 second apart in this region. As a result, we can expect isotropic imaging to provide more reasonable results in this region.

THE ISOTROPIC MIGRATION

To demonstrate the extent to which anisotropy influenced the new Marmousi data set, I isotropically prestack migrate the VTI Marmousi data set. I use the part of the data set with offsets equal or less than 2575 m, which is the limit on the original isotropic data set. This prestack migration, which is based on the Kirchhoff approach to imaging and raytracing for traveltime calculation, is applied using a smooth version on the original velocity model. Figure 8 (top) shows the stacked image after prestack migration on the new anisotropic Marmousi data set. Figure 8 (bottom), on the other hand, shows the result of using this same migration on the original Marmousi data set. I attribute the difference between the two migration results to anisotropy. Although the reservoir appears in both sections, its location is slightly shifted in Figure 8 (top). Also, many of the shallow faults are improperly imaged as a result of ignoring anisotropy. The degradation is far greater on the left side of the section, where the anisotropy is greater, than the right side.

To demonstrate why there are such large differences in imaging, Figure 9 shows common-midpoint gathers after prestack migration for the 4000 m location, which is highly anisotropic. The moveout is better aligned when we apply the isotropic migration to the original Marmousi data set (right) than when we apply the migration to anisotropic data. The difference in Figure 10, for CMP location 8000 m, is far less than what is apparent in Figure 9 which is a result of the reduced anisotropy at location 8000 m as compared to that at 4000 m.

An interesting application of the VTI Marmousi data set is to evaluate what isotropic velocity model would best image the data. This will give us some idea of how much velocity bias anisotropy introduces into the conventional isotropic processing scheme. The synthetic sections (Figure 5) clearly show that anisotropy results in faster traveltimes at the far offsets, and therefore, higher velocities in conventional velocity analysis. These higher velocities, if interpreted as vertical velocities, result in over-estimation of depth, even though δ (the anisotropy parameter responsible for depth mis-ties) is zero for the anisotropic model. Over-estimation of velocity is not

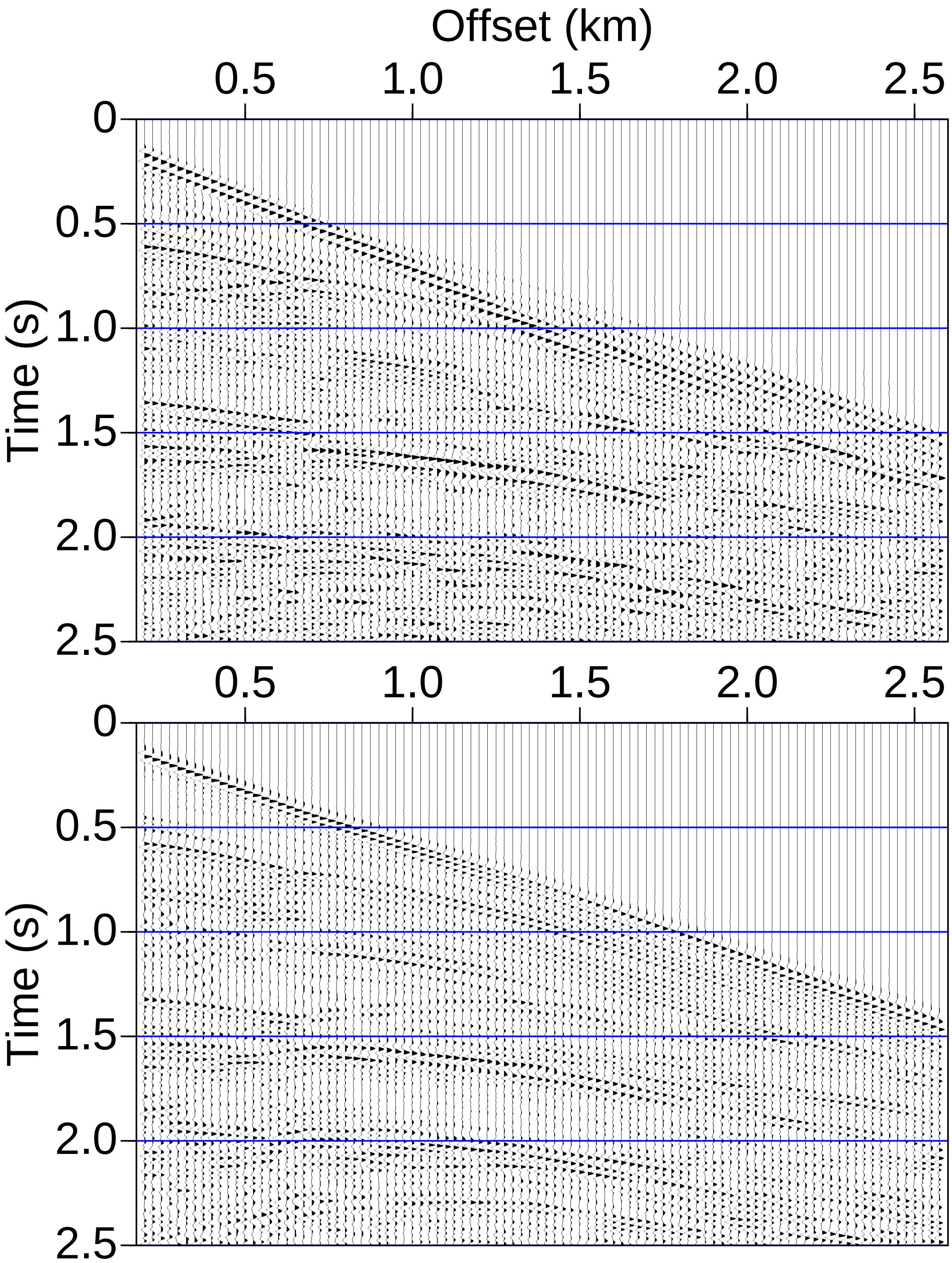

Figure 7: Common-shot gathers, similar to those in Figure 5, but the source is at the 7 km surface location and the geophones span from the 4.2 to 6.8 km locations. Top: Shot gather from the original Marmousi data set, based on an isotropic medium. Bottom: Shot gather based on the VTI model. tariq3-syn-marmo7000 [NR]

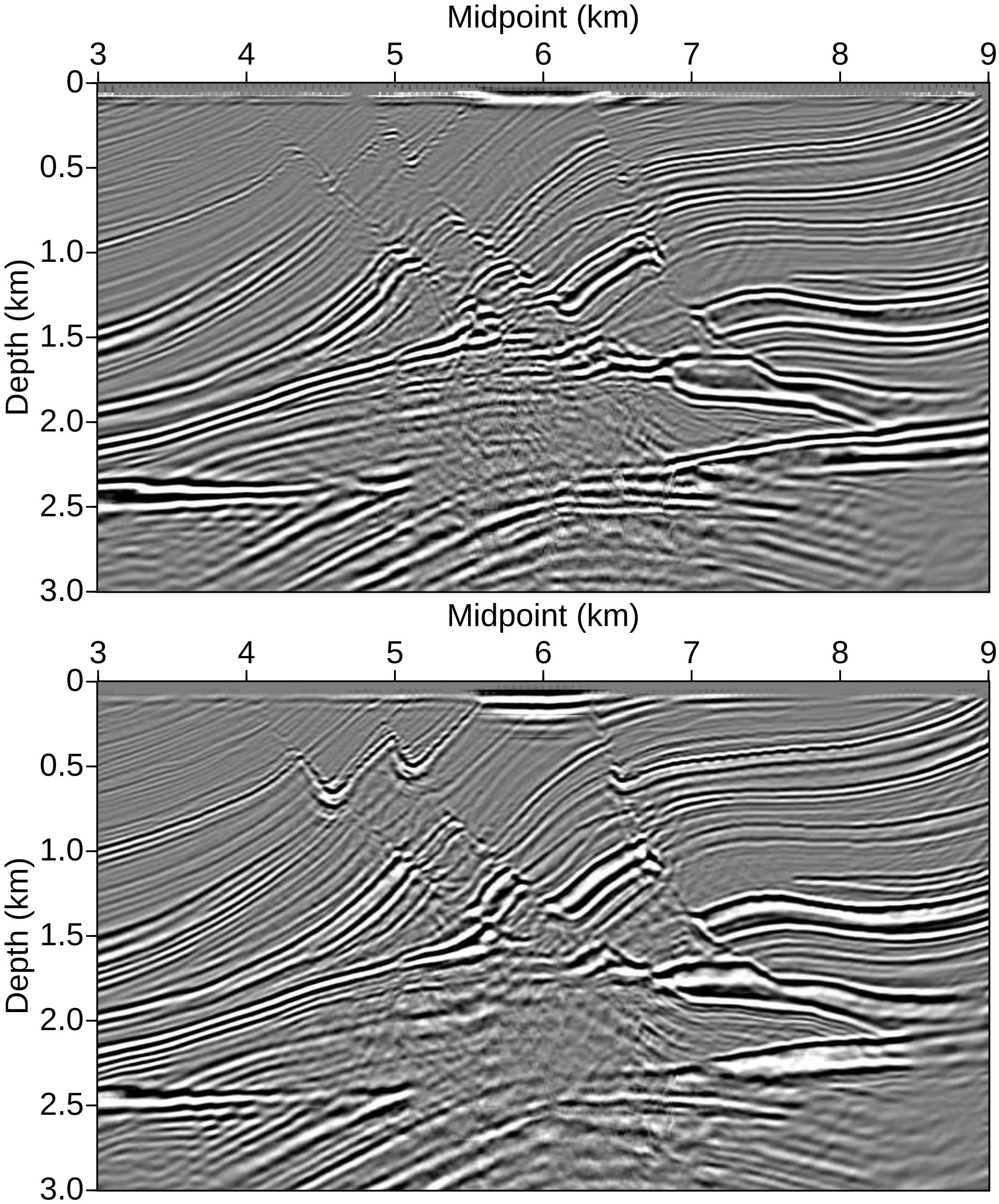

Figure 8: Top: A prestack-migrated section of the anisotropic Marmousi data set, using an isotropic Kirchhoff migration with a smoothed version of the Marmousi velocity model. Bottom: A prestack-migrated section of the original Marmousi data set, using the same isotropic Kirchhoff migration as in top section with the same smoothed Marmousi velocity model. tariq3-marmo-st [NR]

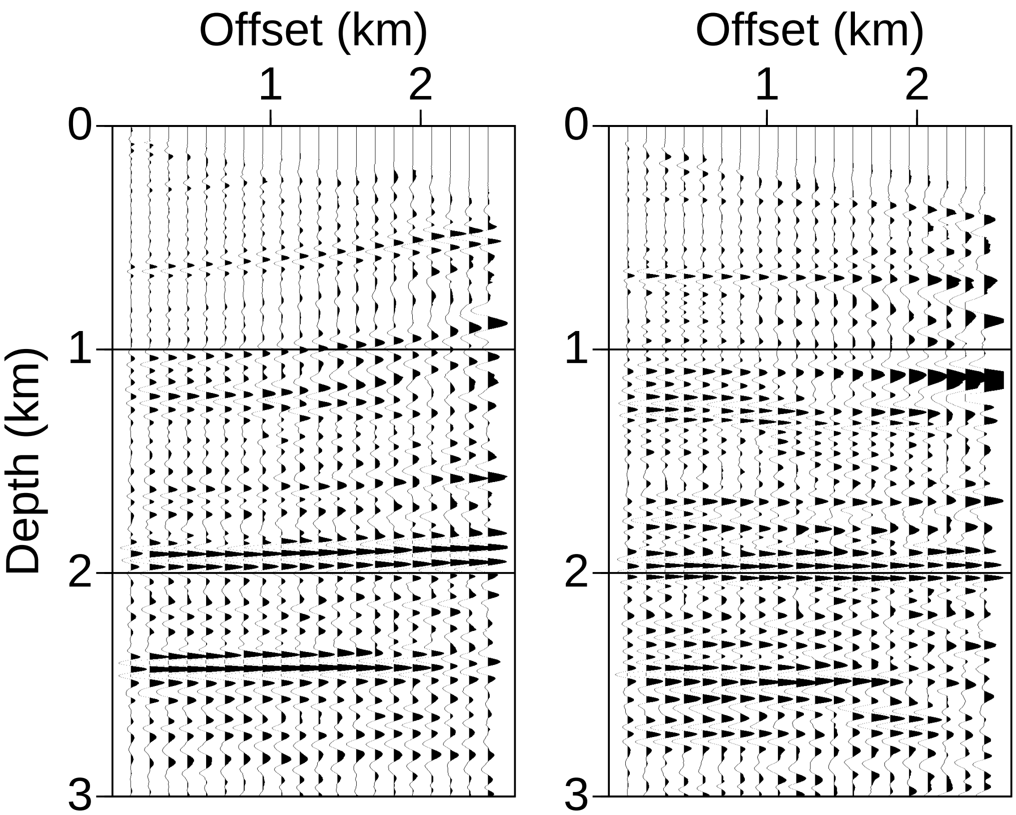

Figure 9: Common-midpoint gathers from the 4000 m location after isotropic prestack migration on the anisotropic Marmousi data set (left), and on the isotropic Marmousi data set (right). tariq3-cmp4000 [NR]

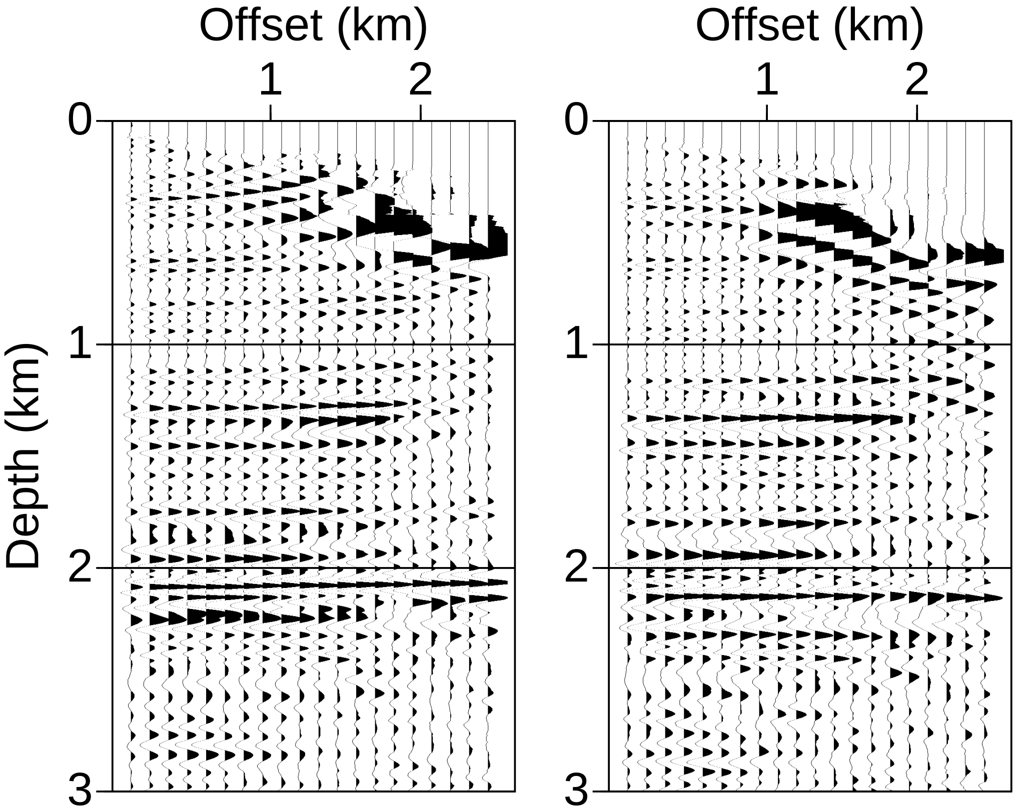

Figure 10: Common-midpoint gathers from the 8000 m location after isotropic prestack migration on the anisotropic Marmousi data set (left), and on the isotropic Marmousi data set (right). $\boxed{\text{tariq3-cmp8000}}$ [NR]

the only problem with the isotropic assumption; both focusing and migration are negatively affected by ignoring anisotropy (Alkhalifah and Tsvankin, 1995).

THE CONCLUSION

Using the acoustic wave equation for VTI media, I generated synthetic data for a transversely isotropic medium in a complex model. This VTI model has an NMO and vertical velocity given by the original Marmousi velocity model. The η model, built with same layering characteristics as the Marmousi velocity model, ranges between 0 and 0.274. The similarity in configuration and acquisition geometry of these VTI Marmousi data and the heavily processed original IFP data simplifies the transport of processing tools to be applied to this new data set. Synthetic sections show the large impact of anisotropy on wave propagation. Anisotropy, for example, results in faster traveltimes at the far offsets. In conventional isotropic processing, such faster traveltimes are often interpreted as higher NMO (and vertical) velocity, and therefore, result in an overestimation of depth.

REFERENCES

Aki, K., and Richards, P. G., 1980, Quantitative seismology: Theory and methods: W. H. Freeman and Co., New York.

Alkhalifah, T., and Tsvankin, I., 1995, Velocity analysis for transversely isotropic media: Geophysics, **60**, 1550–1566.

Alkhalifah, T. A., Fomel, S. B., and Biondo, B. L., 1997, Time-domain anisotropic processing in arbitrarly inhomogenous media: SEP-95.

Alkhalifah, T. A., 1997a, Seismic data processing in vertically inhomogeneous TI media: Geophysics, **62**, 662–675.

Alkhalifah, T. A., 1997b, Velocity analysis using non-hyperbolic moveout in transversely isotropic media: Geophysics, this Nov.-Dec. issue.

Alkhalifah, T., 1997c, Acoustic approximations for seismic processing in transversely isotropic media: accepted for Geophysics.

Alkhalifah, T., 1997d, An acoustic wave equation for anisotropic media: SEP-95.

Audebert, F., Biondi, B., Lumley, D., Nichols, D., Rekdal, T., and Urdaneta, H., 1994, Marmousi traveltime computation and imaging comparisons: SEP–**80**, 47–66.

Banik, N. C., 1984, Velocity anisotropy of shales and depth estimation in the north sea basin: Geophysics, **49**, no. 9, 1411–1419.

Geoltrain, S., and Brac, J., 1993, Can we image complex structures with first-arrival traveltime?: Geophysics, **58**, no. 4, 564–575.

Harris, J. M., Dahlhaus, L., and Michelena, R., 1994, P-wave anisotropy in shales from crosswell data: 64th Annual Internat. Mtg., Soc. Expl. Geophys., Expanded Abstracts, 1125–1128.

Rekdal, T., and Biondi, B., 1994, Paraxial ray tracing in the Marmousi model: 64th Ann. Internat. Meeting, Soc. Expl. Geophys., Expanded Abstracts.

Thomsen, L., 1986, Weak elastic anisotropy: Geophysics, **51**, no. 10, 1954–1966.

Versteeg, R., and Grau, G., 1990, Practical aspects of seismic data inversion, the Marmousi experience 52nd EAEG Meeting, Eur. Assoc. Expl. Geophys., Proceedings of 1990 EAEG Workshop, 1–194.

Versteeg, R., and Lailly, P., 1991, Eaeg workshop report: Practical aspects of seismic data inversion: First Break, **9**, no. 2, 75–80.

Versteeg, R. J., 1993, Sensitivity of prestack depth migration to the velocity model: Geophysics, **58**, no. 6, 873–882.